Advances in Geo-Energy Research

Vol. 11, No. 1, p. 6-19, 2024

Original article

Impact of CO_2 solubility on design of single well tracer tests to evaluate residual saturation during carbon capture and storage

Masra Awag*, Eric Mackay, Saeed Ghanbari

Institute of GeoEnergy Engineering, Heriot-Watt University, Edinburgh EH14 4AS, UK

Keywords:
CO_2 store characterization
residual CO_2 saturation
single well tracer test
partitioning tracer
tracer test design

Cited as:
Awag, M., Mackay, E., Ghanbari, S. Impact of CO_2 solubility on design of single well tracer tests to evaluate residual saturation during carbon capture and storage. Advances in Geo-Energy Research, 2024, 11(1): 6-19.
https://doi.org/10.46690/ager.2024.01.02

Abstract:
Single-well tracer technique have been well applied in many petroleum industry and environmental applications. However, these tests have not been well developed for CO_2 geological storage purposes to evaluate residual CO_2 saturation during the appraisal phase of site investigation, due to the challenges occurring from the complex phase behaviour. In this study, two single-well tracer tests are numerically modelled to quantify the residual gas saturation. Our study addresses the design of an alternative single well tracer test sequence, which involved a single pass of the tracer saturated water over the residually trapped zone, thereby reducing the amount of CO_2 dissolution into the tracer solution. A one-dimensional numerical modelling of the tracer propagation and partitioning with homogenous properties was used for the calculations of the difference in tracer breakthrough times during water withdrawal from the tests. Model sensitivity variations were applied to analyse the impact of reservoir and treatment design parameters on the residual gas saturation. The residual gas saturations calculated reflect the input values, including the effect of hysteresis, to within 10% accuracy. It was found that changing the CO_2 saturated water volume injected after CO_2 made the CO_2 front to travel to different distances from the well, and thus the tracer had different size of residually trapped zones to travel through when it is back produced and encounters different residual gas saturations, and therefore affected the residual gas saturation calculations. The modelling also shows that optimal injection of CO_2-saturated water to prevent the dissolution of the residually trapped CO_2 and establish the residually trapped zone was challenging to achieve, and therefore using the fluid withdrawal method was more robust to establish the residually trapped zone. This is because of the dependency of solubility on pressure. The numerical models may be used to design, optimise, and interpret the field tests.

1. Introduction

The storage of CO_2 in deep geological formations, such as depleted oil and gas fields and saline aquifers, is being studied as one of the various solutions for reducing greenhouse gas emissions and thus to limit climate change related to CO_2 concentration in the atmosphere (Metz and Davidson, 2005). Four trapping mechanisms have been identified for long term geological storage of CO_2, which are known as structural, dissolution, mineral, and residual trapping. These mechanisms have a vital importance in determining how much CO_2 can be stored in geological formations (Metz and Davidson, 2005).

This study focuses on the residual CO_2 trapping process, which occurs during the imbibition stage when the injected CO_2 moves upwards because of buoyancy and the formation water imbibes to refill some, but not all the pore spaces vacated by the displaced CO_2, leaving some disconnected CO_2 ganglia immobilised. The residual trapping is described by a parameter referred to as the residual gas saturation (S_{gr}). This parameter describes the volume of trapped CO_2 in the pore space because of capillary forces relative to the total volume of pore space. It is used to quantify the impact of the residual trapping

Yandy Scientific Press

*Corresponding author.
E-mail address: mma30@hw.ac.uk (M. Awag); e.j.mackay@hw.ac.uk (E. Mackay); s.ghanbari@hw.ac.uk (S. Ghanbari).

Received October 9, 2023; revised October 27, 2023; accepted November 15, 2023; available online November 19, 2023.

process by determining the reservoir capacity to residually trap CO_2. The S_{gr} depends on many factors, including rock type, pore structure, wettability, interfacial tension. For any given rock system, it may vary hysteretically with the sequence of drainage and imbibition processes (Metz and Davidson, 2005).

Although the S_{gr} is very important in determining storage capacity and security, only few studies have tried to quantify it *in-situ*. A comprehensive review of the laboratory, field and numerical model studies focusing on the determination of residual trapping is presented by Krevor et al. (2015). For example, several field scale CO_2 injection projects have been carried out to date, at different sites in United States, Japan and Australia, to demonstrate the existence and stability of residually trapped CO_2 in reservoirs (Krevor et al., 2015).

At the Frio site in Eastern Texas in the United States, near-wellbore observations were performed using a pulse neutron logging saturation tool in the injection and observation wells to estimate residual gas saturation. They utilised cross-well seismic tomography to support these observations, as this technique could cover a bigger region than the neutron logging tool. This analysis gave qualitative information of the plume shape that corresponded well to the saturation profiles in the injection and observation wells (Doughty et al., 2007). At the Nagaoka site in Japan large scale injection was carried out. Neutron, sonic and resistivity logging tools were used for monitoring in the observation wells. Logs were recorded during the injection period, and these measurements were extended for more few years after cessation of injection to determine both the maximum residual gas saturation and the stabilised residual gas saturation (Xue et al., 2006). Two residual trapping experiments were performed in the cooperative research centre for greenhouse gas technologies (CO_2CRC) pilot project at the Otway site in Australia, in 2011 and 2014 (Paterson et al., 2011; LaForce et al., 2014). Various well-testing methods were used in the project. A single injection and production sequence test was performed with five observation techniques to determine the residual trapped CO_2 saturation. These techniques included the use of the pulsed-neutron logging saturation tool (Dance and Paterson, 2016), thermal logging tool, history matching of pressure time series during injection and production (hydraulic pressure test), tracer tests, and a dissolution test. The main concept of the experiments was comparing the well-tests results before and after the residual CO_2 zone was created to measure the residual CO_2 (Paterson et al., 2011; LaForce et al., 2014; Dance and Paterson, 2016).

In the present study, a tracer test technique is used to evaluate the residually trapped CO_2. Tracer testing is the process of injecting one or more tracers into a geological formation to study the flow, transport and reactions of fluids and components in zones that are difficult to access using other methods. This technique can be used for site characterisation prior to CO_2 injection as well as for monitoring and verification reasons during and after CO_2 injection. These tests can be carried out in a single-well injection-withdrawal (push-pull) configuration, at which the tracer is injected and back produced from a single well, or in interwell configurations, which requires using two or multiple wells (Niemi and Bear, 2017). Single-well tracer tests have many advantages that have been mentioned by many researchers; for instance, they are low in costs and need smaller volumes of fluids to be injected and withdrawn compared to (two or multiple) other well tests (Istok et al., 2002; Zhang et al., 2011).

Single-well tracer tests have been well used in many applications, such as (1) in the petroleum industry, where a reactive partitioning tracer that is soluble in water and oil phases has been used, which then formed a second tracer that is only soluble in water and measured the residual oil saturation from the difference in breakthrough curves of the two tracers (Tomich et al., 1973); (2) in environmental applications for remediation, such as for in situ determination of microbial activities or denitrification rates in groundwater aquifers (Kim et al., 2005) and for detecting and quantifying nonaqueous phase liquid contamination in the subsurface (Istok et al., 2002); and (3) for the *in-situ* measurement of soil water content (Nelson et al., 1999) or quantifying the amount of trapped gas in a field-scale infiltration experiment (Heilweil et al., 2004). However, these tests have not been well developed for CO_2 geological storage purposes, due to the challenges occurring from the complex phase behaviour and the variety of trapping mechanisms. Only few carbon capture and storage (CCS)-related studies have used the single well tracer technique for characterising geochemical processes and residual trapping (Matter et al., 2007; Assayag et al., 2009; Zhang et al., 2011; Myers et al., 2012a; Niemi et al., 2020). Some of those studies, which are relevant to the presented work, are discussed below.

Myers et al. (2012a) carried out a single well push-pull tracer test using reactive (ester) partitioning tracer, that can partition between a mobile brine phase and an immobile supercritical CO_2 phase, to estimate the residual CO_2 saturation. The tracer was given time to react and form new tracer with different partitioning properties. Then fluids were withdrawn, and tracer breakthrough curves were recorded to evaluate the residual CO_2 saturation. Their numerical modelling results implied that using ester tracers is a potentially robust technique to quantify CO_2 residual saturation (Myers et al., 2012a). Zhang et al. (2011) designed a single-well injection-withdrawal test using a combination of three tests: Thermal, hydraulic, and partitioning tracer tests, before and after CO_2 injection, to measure the maximum residual gas saturation of supercritical CO_2 in aquifers. The experimental methodology was used to design a practical field test that was carried out as part of the CO_2CRC's Otway project in Australia. Their study reveals that through inverse modelling on synthetic data and with using the combination of the three types of tests and repeating the tests, the uncertainty of the estimated residual gas saturation was reduced (Zhang et al., 2011).

A single well push-pull test was also designed by Paterson et al. (2013), and was used in field tests, again at the Otway project in Australia. Their test design involved using noble gas tracers co-injected with water. During fluid production, different breakthrough signals were produced due to the different partitioning behaviour of the tracers. The residual CO_2 saturation was calculated using the differences in partitioning and comparison to the case of no partitioning (when no immobile is

CO_2 present in the system). The numerical simulations results presented by Paterson et al. (2013) revealed the dependency of the residual gas saturation on the initial gas distribution. At the areas where a higher initial gas saturation was obtained, a greater residual gas saturation was achieved (Paterson et al., 2013).

Following the same theory suggested by Zhang et al. (2011) and the first Otway experiment, Rasmusson et al. (2014), designed and compared three alternative single well tests sequences to evaluate the residual CO_2 saturation. Results from this work were used to develop a test design for the Heletz pilot injection field experiments to determine CO_2 residual trapping *in-situ* (Niemi et al., 2016). Their test sequence involved three stages. The first stage involved carrying out thermal, hydraulic and tracer measurements before CO_2 injection. In the second stage, two approaches were carried out to create the residual CO_2 zone. In the first approach, CO_2 was injected followed by water saturated CO_2 injection to push CO_2 further into the formation and establish the residual trapped zone. In the second one, CO_2 was injected and produced back until a zone of residual CO_2 saturation was created. The third stage included performing hydraulic, thermal and tracer measurements after the residually trapped CO_2 zone was established. The study investigated a new alternative way for establishing the residually trapped zone using withdrawal and an indicator-tracer approach. The indicator tracer, which is a non-reactive tracer that stays in the aqueous phase, was used to identify the point in time when the residually trapping condition was reached in the reservoir when establishing the residual trapped zone through withdrawal. They also used a dissolved gas partitioning tracer, which can partition between the gaseous and aqueous phases, resulting in different tracer breakthrough curves with the difference in arrival times for the tracer tests performed at residual gas conditions and fully-water saturated conditions, to evaluate the residual CO_2 trapping. Numerical modelling results indicated that the residually trapped zone could be established using the indicator-tracer approach without increasing the uncertainty in the evaluation of S_{gr}. The uncertainty in the S_{gr} was also reduced through using the additional pressure measurements from a nearby passive observation well (Rasmusson et al., 2014).

Niemi et al. (2020) performed two field experiments at the Heletz pilot CO_2 injection site using two different methods and a combination of hydraulic, thermal and tracer tests to evaluate the residual trapping of CO_2 *in-situ*. Joodaki et al. (2020a, 2020b) carried out numerical modelling with TOUGH2/ECO2N to interpret the whole test sequence of these experiments, with the main objective of obtaining an *in-situ* S_{gr} value. In the first experiment, hydraulic withdrawal tests were performed before and after establishing the residually trapped CO_2 region to measure the response of the formation pressure when no CO_2 is existing in the formation and comparing it to the response of pressure when there is the residually trapped CO_2, to estimate the residual gas saturation in the formation. The residually trapped zone in the first experiment was established by injecting supercritical CO_2 and then producing the mobile CO_2 from the formation and leaving behind the residual CO_2 (Niemi et al., 2020). In the second experiment, two tracer tests were performed by injecting a gas partitioning tracer prior to and after creating the residual CO_2 zone. Then the tracer was withdrawn and the difference in tracer recovery from the two tests gave an estimation of the residual CO_2 saturation in the system. In the second experiment the residual CO_2 zone was established by injecting supercritical CO_2 followed by CO_2-saturated water injection to push the mobile CO_2 away, leaving behind the residual CO_2. Niemi et al. (2020) found that the hydraulic withdrawal test is a robust procedure for measuring the residually trapped CO_2. However, the hydraulic test has limitations in which it only produced an average value (an effective residual gas saturation) over the whole test section. The tracer tests were more complicated to perform and required sensitive equipment; however, they provided thorough information about the residual CO_2 distribution in the system than the hydraulic tests. The optimal injection of CO_2-saturated water to prevent the dissolution of the residually trapped CO_2 was challenging to achieve, and therefore using the fluid withdrawal method was more robust to create the residual CO_2 zone.

Since only few studies in the literature have considered carrying out single-well push-pull tracer tests in CCS related projects to evaluate residual trapping, the study presented in this paper addresses the design and modelling of an alternative single well tracer test sequence that may produce additional valuable information on quantifying the residual trapping of CO_2. The study follows the main concept of the single well tracer tests suggested by Zhang et al. (2011), Paterson et al. (2013), Niemi et al. (2020) and the Otway experiments, in which two single-well injection withdrawal tracer tests are carried out using gas partitioning tracer to evaluate the residual gas saturation. However, the design of the test sequences of our study is completely different compared to previous studies. The main variation in our test design is the stage of establishing the residual CO_2 zone in the formation. This is created after the partitioning tracer is injected into the system, while in the previous studies (e.g., Zhang et al. (2011)), the residual CO_2 zone was established prior to injection of the tracer. Our design involved a single pass of the tracer saturated water over the residual CO_2 zone, thereby reducing the amount of CO_2 dissolution into the tracer solution, which may give clearer results in determining the residual gas saturation. In previous studies there were two contacts between the tracer and the residual CO_2 zone, since the tracer passed through the residual trapped CO_2 twice, i.e., during injection and production stages.

The second variation is the method of establishing the residual CO_2 zone in the formation. This is created by first injecting a small amount of CO_2-saturated water before free phase CO_2 injection, to limit the dissolution of CO_2 during the back production of the tracer and then, withdrawing the mobile CO_2 back, to create the residually trapped zone. Our method limits the dissolution in the trailing and leading edges of the CO_2 slug during the injection stages. It also limits the dissolution of the residual CO_2 during the back production stage. However, in preceding studies they either used the CO_2-saturated water injection method after CO_2 injection (Paterson et al., 2013; Niemi et al., 2020) or the fluid withdrawal meth-

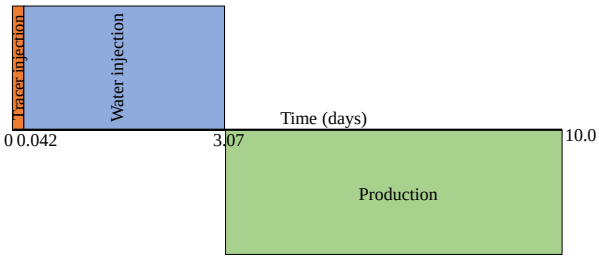

Fig. 1. Schematic diagram of the first tracer test sequence.

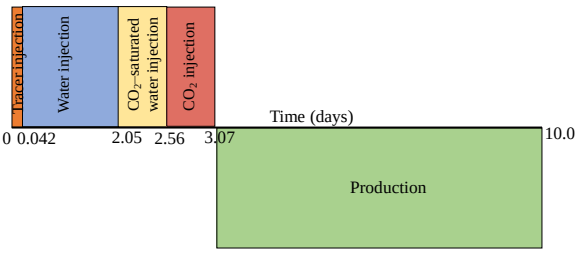

Fig. 2. Schematic diagrams of the second tracer test sequence.

od to establish the residual CO_2 zone (Zhang et al., 2011; Rasmusson et al., 2014; Niemi et al., 2020). These studies have not considered injecting CO_2 saturated water before the CO_2 to reduce the dissolution of CO_2, but only considered injecting CO_2-saturated water after free phase CO_2 injection for the purpose of establishing the residual CO_2 zone (Zhang et al., 2011; Rasmusson et al., 2014; Joodaki et al., 2020a, 2020b; Niemi et al., 2020). The third alteration in our test is that a rest (soaking) period was not implemented after the tracer injection because, as the tracer was injected before the establishment of the residual trapped CO_2 zone, it would have enough time to soak and partition into the trapped CO_2 during back-production. In previous studies (Joodaki et al., 2020a, 2020b; Niemi et al., 2020) a soaking period was included following the tracer injection, to allow the tracer water mixture to soak and partition into the immobile gas (CO_2) phase and become immobile before producing fluid back and measuring tracer concentrations. The last alteration in the test design included injecting chase-water after the tracer and before CO_2 injection, which worked as a barrier between the tracer and free phase CO_2, to ensure there is no mixing between the tracer and CO_2 during the injection stages.

This study addresses the estimation of residual CO_2 saturation in the presence of brine only and does not consider the presence of other phases, and therefore it is applicable for CO_2 residual saturation estimation in aquifers. Overall, the first tracer test involved injecting a dissolved noble gas, Xenon, tracer into a fully water-saturated reservoir, and then water is injected continuously to push the tracer further away from the injection well before pulling it back to the borehole by turning the well to production, to measure the tracer breakthrough curve. It should be mentioned that other noble gases, such as Krypton, can also be used for the purpose of this study, as it is chemically similar to Xenon. Nobel gas was proposed to be used in this test because (1) it can partition between the aqueous and CO_2-gaseous phases, (2) it is chemically inert gas and unhazardous, (3) it can be measured with precision (Zhang et al., 2011), and (4) it has limited interaction with the reservoir rocks and formation water (Myers et al., 2012b). The same procedure is performed in the second test, but with added extra steps. In this latter case, after the tracer is co-injected with water and followed by CO_2-saturated chase-water injection, supercritical CO_2 is then injected. During fluid production the tracer breakthrough curve is measured. The residual gas saturation in the reservoir may affect the tracer breakthrough and recovery curves because part of the tracer partitions into the residually trapped gas and becomes immobile, and therefore will not be produced back as fast as in the first tracer test. The residual gas saturation can be estimated from the difference between breakthrough curves from the first and the second tracer tests (Zhang et al., 2011).

The structure of this paper is as follows: In Section 2 the methodology including the experimental sequence and the numerical simulation models that are utilised to model the experimental sequence, are discussed. In Section 3 the results for the simulation modelling are discussed. Section 4 presents a discussion for the base case models and sensitivity variations to the base case model. Finally, Section 5 outlined the conclusions.

2. Methodology

A single-well injection production tracer test is designed and modelled, in which the same well is used for fluid injection and production.

Two numerical experiments have been carried out to quantify the residual gas saturation. Descriptions of the experiment sequence, simulation model, fluid properties and relative permeability functions that are applied to create the tracer tests are discussed in the following section.

2.1 Experiment sequence

The main concept of the two experiments is to use a noble gas partitioning tracer with and without the creation of the residual CO_2 region to determine the amount of residual CO_2 saturation in the system. The overall sequences of the first and second tests, including the duration and injection and production rates, are given in Tables 1 and 2, respectively. Schematic diagrams of the first and second test sequences are presented in Figs. 1 and 2, respectively. Each part of the two tracer experiments is discussed below in detail.

2.1.1 First tracer experiment

In the first tracer experiment, gas partitioning tracer Xenon is co-injected with water when the pore space was fully saturated with formation water, and no CO_2 is present in the formation. Other noble gases tracers such as Krypton can also be used for the study as it is chemically similar to Xenon. Tracer injection is started and continued for about 0.042 day (1 hour). Untraced water injection has then started after the tracer injection stage, to push the Xenon away from the injection zone, which continued for about 3 days. Then fluids are produced back to measure the tracer recovery curve, and the production lasted for about 7 days.

Table 1. Sequence for the first tracer test with downhole injection production rate of 10 m^3/day.

Test 1 steps	Description	Duration
1	Tracer injection	1 hour
2	Chase water injection	3 days
3	Fluid production	7 days

Table 2. Sequence for the second tracer test with downhole injection production rate of 10 m^3/day.

Test 2 steps	Description	Duration
1	Tracer injection	1 hour
2	Chase water injection	2 days
3	CO_2 saturated water injection	0.5 days
4	CO_2 injection	0.5 days
5	Fluid production	7 days

2.1.2 Second tracer experiment

In the second tracer experiment, Xenon was co-injected with water into the reservoir, again for 0.042 days. This was followed by untraced water injection, which continued for 2 days. To push the tracer away from the injector to the same distance as for the first tracer experiment, but to also ensure that a CO_2 saturated zone is established between the well and the injected tracer, CO_2-saturated water was then injected for 0.5 day, followed by supercritical CO_2 injection for 0.5 day to saturate the near wellbore region with CO_2. The *downhole* injection rate for all stages is maintained constant at 10 m^3/day, so by the end of the day 3 of injection after the tracer itself has been pumped, the same volume of fluid has been injected in both cases. It should be mentioned that the water injected after the Xenon and before the CO_2 also acts as a barrier between the Xenon and the CO_2 to ensure there is no mixing between Xenon and CO_2 during the injection stages. The next step is the establishment of the residual CO_2 zone. The CO_2-saturated water that was injected for 0.5 days before CO_2 injection, was just enough to limit the dissolution of the injected CO_2 into water contacted. Withdrawing the mobile CO_2 back would lead to this CO_2 saturated water sweeping the mobile gas phase CO_2 and leaving the residually trapped CO_2 behind. To produced back all the fluids, including the tracer, the production started from day 3 after the end of tracer injection, and lasted for 7 days, as in the first tracer experiment. During fluid production the tracer breakthrough and subsequent curve is calculated.

The main concept of the second test is that the residual CO_2 zone in the system will have an impact on the tracer breakthrough time and recovery curves. This is because the tracer partitions into the gas in the residual CO_2 zone and part of the tracer is trapped with the CO_2 and will not be recovered during back production as fast as in the first tracer test. In other words, there will be a delay in tracer production as the presence of the residually trapped CO_2 retards the tracer recovery. The shape of the tracer recovery curve will be affected, as well as breakthrough time and time for the arrival of the peaks. The residually trapped CO_2 (residual gas saturation) is estimated from the difference in tracer recovery from the first and second tracer tests (Zhang et al., 2011).

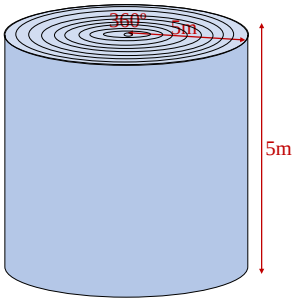

Fig. 3. A schematic diagram of the numerical 1D mode. There are 1,000 cells in the radial direction (shown schematically here), each D_R = 0.005 m (D_R assigns grid block sizes in the radial direction).

2.2 Numerical simulation model description

The two single well tracer experiments are modelled using the compositional simulator CMG-GEM (CMG, 2020). Two phases, which are the CO_2-rich 'gaseous' phase, and the brine-rich 'aqueous' phase, are included in the simulation model. Equilibrium phase partitioning of Xenon and CO_2 between the gaseous and aqueous phases is assumed. CO_2 and Xenon solubilities in water are evaluated using Henry's law. Henry's coefficient for Xenon is 3.8×10^6 kPa at 64 °C (Joodaki et al., 2020a, 2020b). The model is composed of CO_2, Xenon, and dissolved NaCl in the water phase. All simulations are performed under isothermal conditions.

A one-dimensional (1D) numerical radial compositional modelling consisting of 1,000 grid blocks and homogenous properties is used for the calculations, thereby making the study simpler. More complex two-dimensional and three-dimensional models including heterogeneity will be used in future work to assess the impacts of heterogeneity, capillary pressure, and gravity effects. The radial extent is 5 m in the horizontal direction and 5 m grid blocks are used in the vertical direction. The diameter of 5 m is a typical distance that a tracer might be injected to. The test volumes are on purpose relatively small, because there is no advantage in using larger volumes. Injecting a tracer at greater distance would involve larger volume of fluid and require more time, and there would be no additional information gained but the cost would increase. In addition, very large cells are added at the outer boundary of the model through a pore volume multiplier to provide a constant pressure outer boundary condition, so there is no unrealistic pressure build up in the near wellbore region.

The model has a single well, with this same well being used for fluid injection and production. The well is placed in the centre of the model. A schematic figure of the numerical 1D radial model is illustrated in Fig. 3. The parameter values

Table 3. Input parameters of the model.

Parameters	Value
Grid	1,000 × 1 × 1
Model size (R, θ, Z)	5 m × 360° × 5 m
Grid block size (D_R, D_θ, D_Z)	0.005 m× 360° × 5 m
Wellbore radius	0.1 m
Initial pressure at reference depth	14,500 kPa
Temperature (isothermal)	64 °C
Reference depth	2,000 m
Permeability	400 mD
Porosity	0.25 (-)
Well flow rate (at reservoir conditions)	10 m^3/day
Tracer concentration in water phase (C_w)	1.71 mg/L
Tracer concentration in gas phase (C_g)	8.08 mg/L
Partition coefficient ($K = C_g/C_w$)	4.72 (-)

used in the numerical modelling are presented in Table 3 below. The initial conditions were chosen to be the same as the one used in previous studies by Joodaki et al. (2020a, 2020b) and Niemi et al. (2020).

Fig. 4 shows the relative permeability functions for water (K_{rw}) and gas (K_{rg}) versus water saturation. Corey's correlation for a two-phase water-gas system is used to obtain the relative permeability curves. The connate water saturation is assumed to be (S_{wc} = 0.3). Hysteresis is considered in the relative permeability model as shown in Fig. 4 below. The residual gas saturation after hysteresis is S_{gr} = 0.2 for the base case model. Capillary pressure is not modelled explicitly at this stage for the sake of simplicity in interpretation of the results.

3. Simulation results

The modelling results for the base case model and the various model sensitivity variations applied to this base case model are presented here. The results of the two experiments are compared before and after the establishment of the residual CO_2 zone to provide an evaluation of the residual CO_2 saturation using the following equation (Tomich et al., 1973; Zhang et al., 2011):

$$S_{gr} = \frac{t_2 - t_1}{t_2 - t_1 + K(t_1 - t_0)} \quad (1)$$

where t_1 and t_2 are the times elapsed (in days) between the well being put on production and the peaks in the tracer return curves for the partitioning tracer from the first and second experiments, respectively. t_0 denotes the tracer backflow start time. $K(C_g/C_w)$ is the gas to water partition coefficient, which is defined as the ratio of the Xenon concentration in the gaseous phase (mg/L) to the Xenon concentration in the aqueous phase (mg/L).

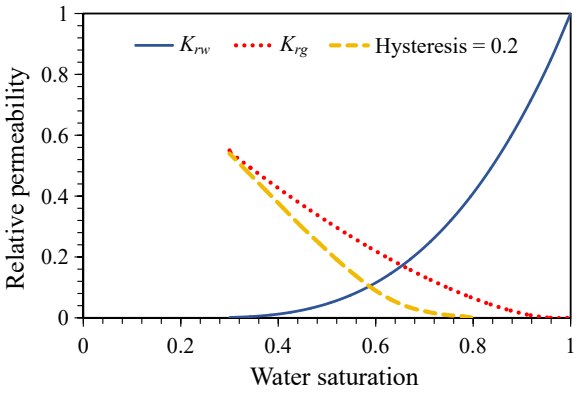

Fig. 4. Gas and water relative permeability as a function of water saturation used in the modelling study.

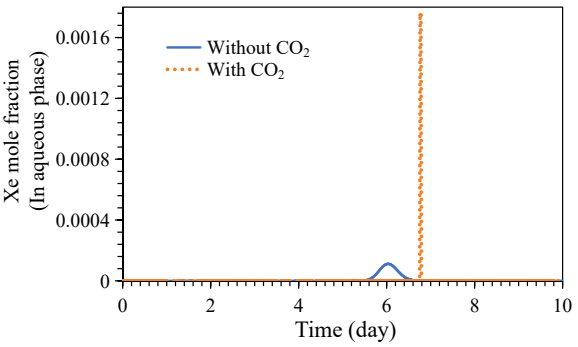

Fig. 5. A schematic diagram of the numerical 1D mode. There are 1,000 cells in the radial direction (shown schematically here), each D_R = 0.005 m (D_R assigns grid block sizes in the radial direction).

3.1 Base case model

As noted above, the base case model includes two experiments, the first of which is of tracer injection into a fully water saturated reservoir, where there is no CO_2 presented in the formation. The total amount of the injected Xenon is 4.14 kg, which is co-injected with 0.42 m^3 of water.

Untraced water was then injected after the Xenon injection and continued for 3 days, with the total amount of injected water being 30 m^3. This amount of water is just enough to push the Xenon away from the injection zone and leave a 2.5 m zone into which the CO_2 may be injected in the second test, without there being any possibility of CO_2 and Xenon mixing during the injection stage (in the second test). A total of 70 m^3 of water and all the injected 4.14 kg of Xenon are then produced.

In the second tracer experiment, the total amount of Xenon injected is the same as in the first tracer test, 4.14 kg. Tracer injection is then followed by water injection for 2 days to push the Xenon away from the injection zone.

Then the additional stage was modelled, which is the creation of the residually trapped zone by first injecting CO_2-

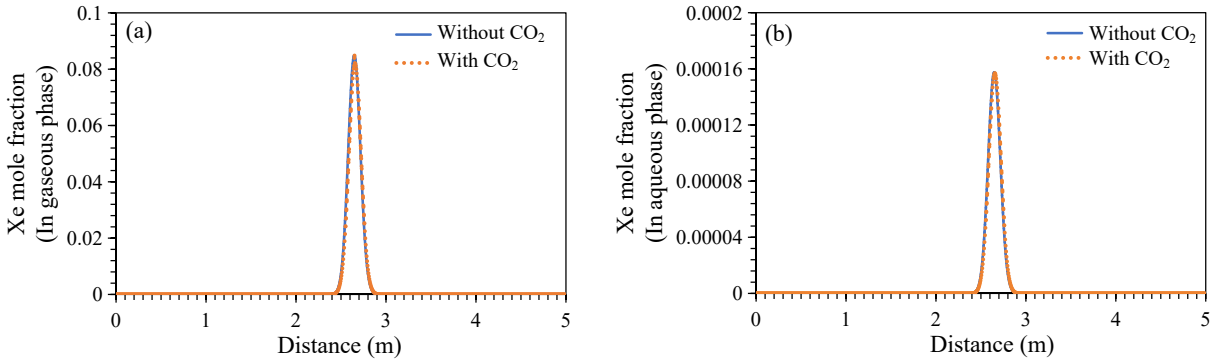

Fig. 6. Tracer mole fraction in the (a) gaseous and (b) aqueous phase at the end of the injection stages versus distance for the base case of the two tracer tests.

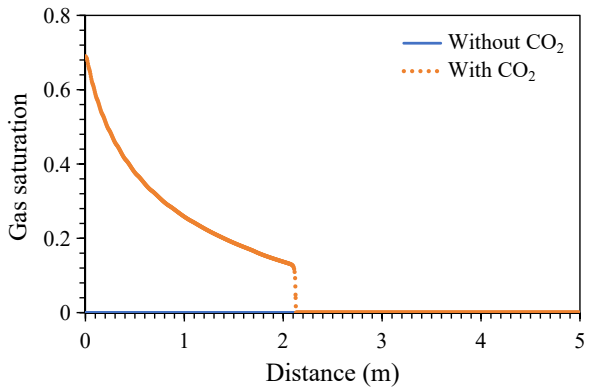

Fig. 7. Gas saturation versus distance at the end of injection stage for the two tracer tests.

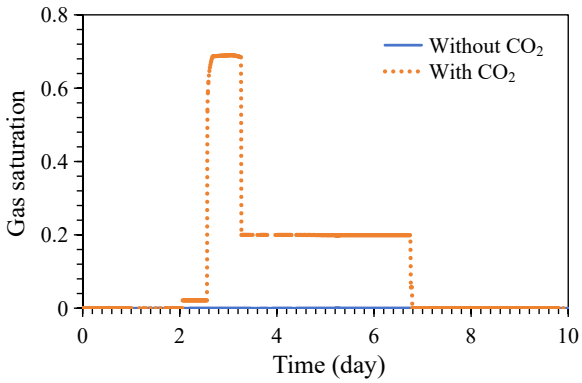

Fig. 8. Gas saturation in the first grid block versus time for the base case of the two tracer tests.

saturated water for 0.5 days to prevent or limit the dissolution of the leading edge of the CO_2 slug, before the supercritical CO_2 is itself injected. Injection of CO_2-saturated water also limits the dissolution of the residually trapped CO_2 during the back production stage.

The tracer arrival times at the well are presented as tracer concentrations in the aqueous phase versus time in Fig. 5. The time of arrival of the tracer peaks for the two tests may be identified from Fig. 5 to calculate the residual gas saturation using Eq. (1).

Note that the shape of the tracer recovery curve as well as the arrival of the peaks are affected by the presence of the residually trapped CO_2 (Fig. 5). In the absence of a residual CO_2 phase, the tracer return curve follows a typical bell-shaped curve, reflecting the amount of dispersion in the system. However, in the presence of a residual CO_2 phase, the tracer breakthrough is retarded, and the tracer recovery is concentrated into a short time interval, leading to a very sharp peak in the recovery function. The presence of residual CO_2 has a very clear and distinctive impact on the tracer recovery profile.

The tracer mole fraction in the gaseous and aqueous phases as a function of distance at the end of the injection stages are shown in Figs. 6(a) and 6(b), respectively. Note that in both cases, the profiles overlie exactly for both aqueous and gaseous phases. This demonstrates that the volume of chase water, CO_2 saturated water and CO_2 injected in the second test match exactly the volume of chase water injected in the first test. Furthermore, it is noted that in each grid block at each time step the concentrations of the tracer in the aqueous and gaseous phases are exactly in equilibrium.

Gas saturation at the end of the injection stage as a function of distance, for a system with a specified maximum residual gas saturation of 0.2 (assuming hysteresis), is shown in Fig. 7. The gas saturation as a function of time in the first grid block (closest to the well) for the same system is shown in Fig. 8. In regions where CO_2 injection has driven the water saturation down to its irreducible saturation and there has been sufficient CO_2 volume throughput, the gas saturation is close to the 0.7 value, which is the maximum gas saturation delineated by the drainage curve (as can be seen in Fig. 8, between the well and 0.025 m from the well).

In the region closest to the well-i.e the first grid block (Fig. 7)-during fluid withdrawal, when the mobile CO_2 was withdrawn back leaving behind the residually trapped CO_2, the gas saturation is driven down to the residual value of 0.2. At the part of the CO_2 saturated zone furthest from the well (ca. 2.125 m), the water saturation may not have been driven down to irreducible water saturation due to insufficient volume throughput of CO_2, and so the hysteresis function will define

Table 4. A summary of the sensitivity study parameters.

Critical gas saturation (after hysteresis)	CO_2 saturated water injected after CO_2 injection (hours)
0.2	/
0.3	/
0.4	/
0.2	/
0.2	0.3
0.2	3.0
0.2	12.0

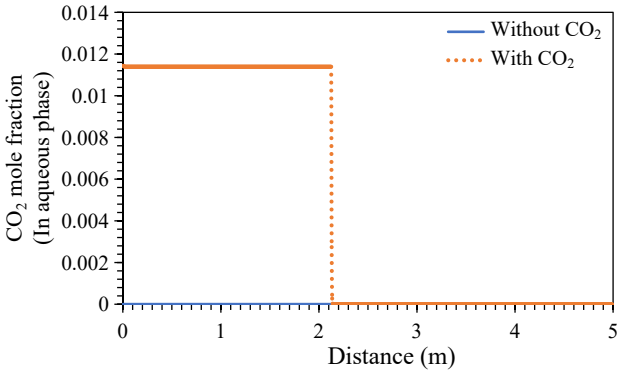

Fig. 9. CO_2 water mole fraction versus distance at the end of injection for the two tracer tests.

a residual gas saturation lower than 0.2-i.e. somewhere between the residual saturations defined by the imbibition curve (0.2) and that defined by the drainage curve (0).

Fig. 9 illustrates the CO_2 water mole fraction versus distance at the end of injection stages. Wherever CO_2 is present as a free phase gas, the water is fully saturated with CO_2, since the dissolution is an equilibrium process, and depends on pressure, temperature, and salinity, but not on the gas saturation, provided it is finite.

3.2 Sensitivity analysis

Various sensitivity calculations were carried out to analyse the impact of reservoir and treatment design parameters on the residual gas saturation calculations from the two tracer tests. Important parameters that can affect the time taken for the peaks in tracer recovery to be reached, and hence the calculated residual gas saturation, include the variation in the input hysteresis value and the volume of chase CO_2 saturated water injected after the CO_2 injection stage. A summary of the sensitivity study parameters is presented in Table 4. The results of the sensitivity studies are discussed in detail in the following.

3.2.1 Change in critical gas saturation value after hysteresis

Sensitivity to the critical gas saturation value after hysteresis was calculated. Three hysteresis values (S_{gr} = 0.2, 0.3 and 0.4) are used as inputs in the simulator to identify their effect on the residual gas saturation calculations.

Table 5. The calculated residual gas saturations with changing the critical gas saturation after hysteresis value.

K	t_1 (day)	t_2 (day)	Hysteresis (input) S_{gr}	Calculated S_{gr}
4.72	6.07	6.77	0.2	0.198
	6.07	7.27	0.3	0.298
	6.07	7.90	0.4	0.393

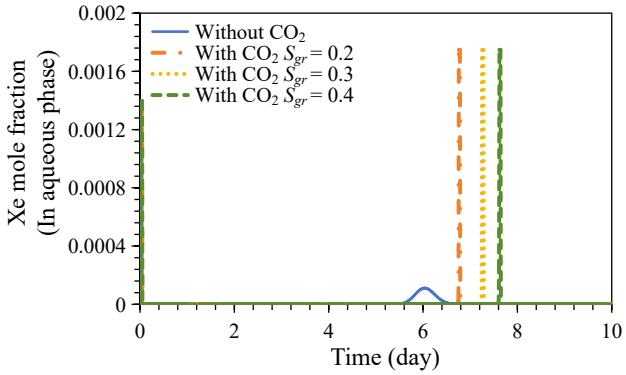

Fig. 10. Tracer concentration in the aqueous phase versus time for the two tracer tests at the well with changing hysteresis value.

The plot in Fig. 10 reveals the tracer concentration in the aqueous phase versus time with changing the value of critical gas saturation after hysteresis. The results in Table 5 present the calculated residual gas saturations, which are determined using Eq. (1).

The first observation is that the higher the maximum residual gas saturation entered in the hysteresis function, the greater the retardation of the tracer when it is produced. The second observation is that the application of Eq. (1) in these various sensitivity calculations yields a calculated residual gas saturation that is within 10% of the input hysteresis value.

3.2.2 Change in the amount of chase CO_2 saturated water injected

Next, four different scenarios were considered in which the volume of the CO_2 saturated water injected after the CO_2 was varied. In the first scenario CO_2-saturated water was not injected after the CO_2. The second scenario included injection of a very small amount of CO_2 saturated water for about half an hour. In the third scenario, CO_2 saturated water was injected for 3 hours. In the last scenario CO_2 saturated water was injected for 12 hours. Figs. 11(a)-11(d) illustrate the gas saturation versus distance for these various sensitivities, including the change in hysteresis value as well as the amount of the CO_2 saturated water injected after CO_2 injection.

In the region closest to the well, during the CO_2-saturated water injection the gas saturation is first driven down to this residual value of 0.2, 0.3 or 0.4, but then it drops further

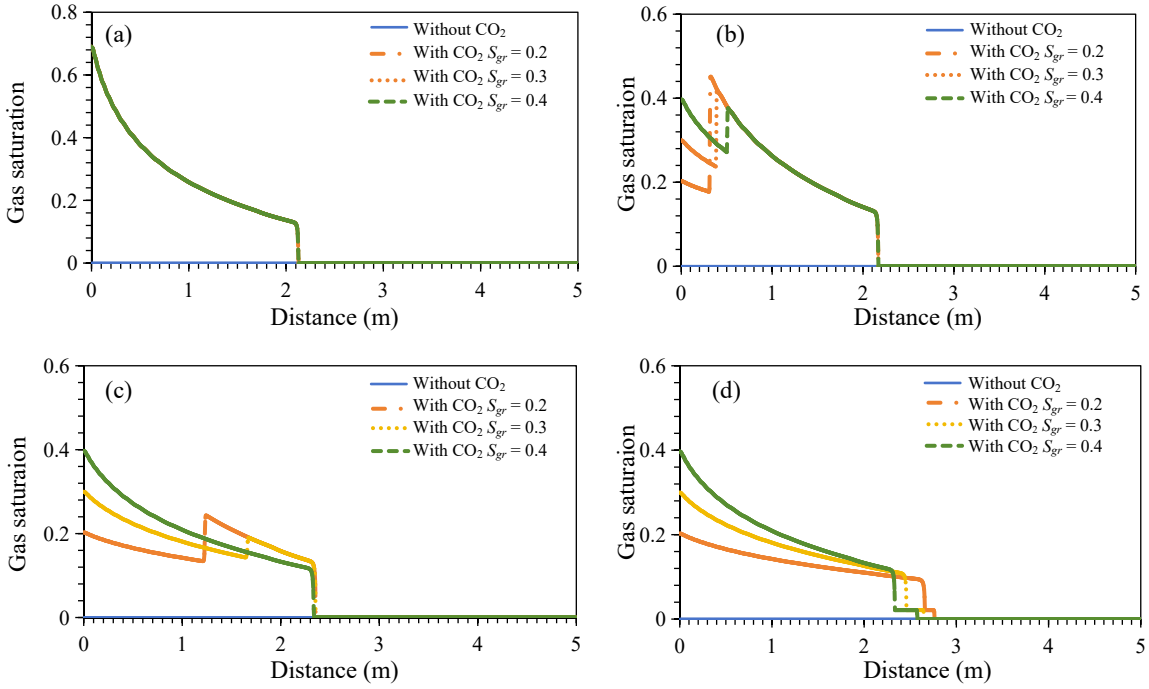

Fig. 11. Gas saturation versus distance at the end of injection for the second tracer test with change in hysteresis value and CO_2-saturated water injection: (a) Without injecting, (b) 30 minutes, (c) 3 hours and (d) 12 hours.

to below the residual saturation values. This is due to the dependency of the residual gas saturation on the initial gas distribution (saturation). The higher the initial gas saturation, the greater the residual gas saturation. At distances closest to the well as the rock volume is smaller than at 5 m, there has been sufficient volume throughput of CO_2 injection, so the rock has reached the maximum gas saturation defined by the drainage curve (0.7), and therefore greater residual saturation values are obtained during the CO_2-saturated water injection stage. In the region furthest from the well, the gas saturation has not reached the maximum value and water saturation has not been driven down to its irreducible saturation value due to insufficient volume throughput of CO_2, and so the hysteresis function will define a residual gas saturation value lower than 0.2, 0.3 or 0.4. This behaviour explains why, in Figs. 11(b)-11(d), there is a region of gas saturation below the value defined in the input hysteresis data (0.2, 0.3 and 0.4, respectively). In Fig. 11(b) from 0.3 to 1.3 m there is a region of gas saturation above the residual values: here there will have been insufficient chase CO_2 saturated water throughput to drive the gas saturation down to the residual saturations.

For Eq. (1) to be applied effectively, it would be expected that as much as possible of the pore space between the tracer and the well should be at a (uniform) residual gas saturation. It may be noted that since the residual gas saturation is associated with the chase CO_2-saturated water imbibition displacement process, variations in the input hysteresis value of residual gas saturation affect the trailing, not the leading edge of the gas slug. The higher the input hysteresis value of residual gas saturation, the higher the gas saturation at the trailing edge. However, this also leads to a lower gas saturation in the centre of the slug, if the gas in the centre of the slug is mobile, which it is in Figs. 11(b) and 11(c), but not in Fig. 11(d). It may be observed that it is in fact quite difficult to achieve a uniform gas saturation in the zone between the tracer and the well. Part of the reason, as has been noted already, is that the residual gas saturation is in fact not constant and changes with distance and it depends on the initial gas saturation, and since in a radial system the rock volume is not the same everywhere, therefore the gas saturation will not be uniform.

Figs. 12(a)-12(d) show the mole fraction of CO_2 in the aqueous phase versus distance at the end of the injection stages, with sensitivities to the changes in the volume of chase CO_2 saturated water injected after the CO_2 injection.

Once again, wherever there is free phase CO_2 present, the water will be saturated with CO_2, as comparison between Figs. 12(a)-12(d), and between Figs. 11(a)-11(d) show.

4. Discussion

4.1 Base case model

The results illustrated in Fig. 5 indicate that part of the tracer from the second tracer test has partitioned into the CO_2 phase. The tracer breakthrough curve is sensitive to the input hysteresis residual gas saturation because the tracer that is partitioned into the gas becomes immobile and will not be produced back at the same time as the water in which it was originally dissolved is produced. As a result, the tracer arrival is delayed in the second test relative to the arrival time in the first test. These findings show that our design method agree with previous studies (e.g., Zhang et al. (2011)).

According to the plots in Fig. 6, which present the tracer

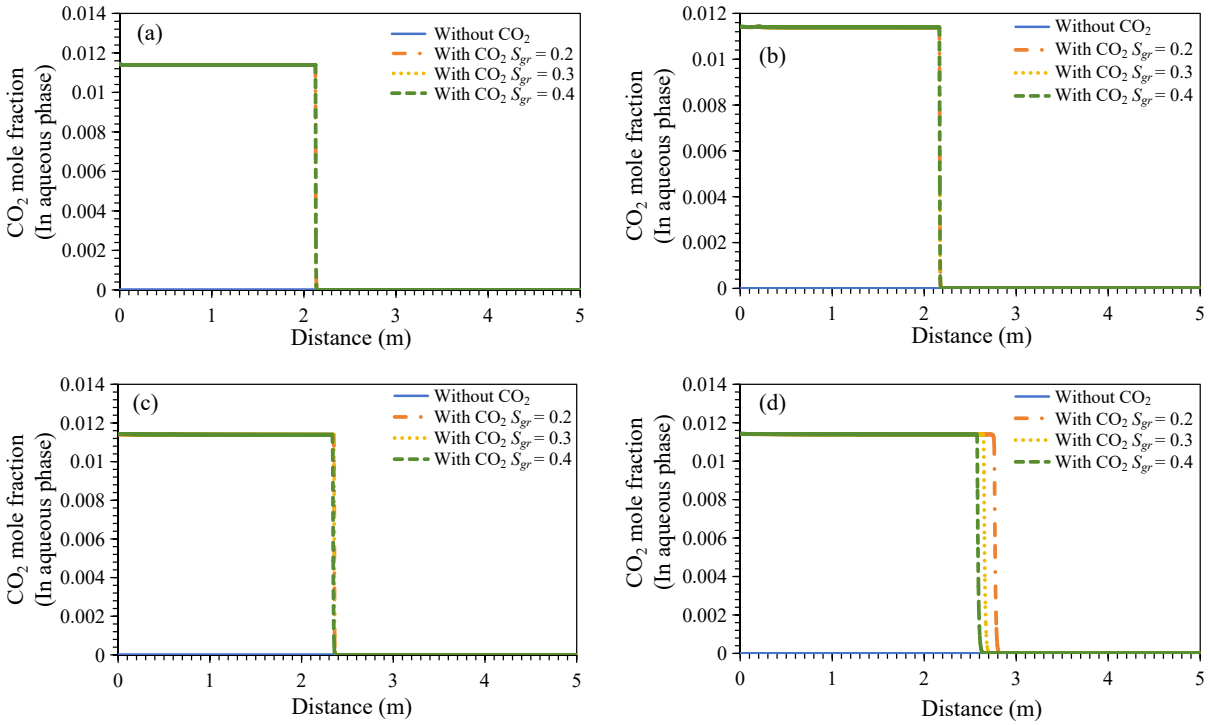

Fig. 12. CO_2 water mole fraction versus distance at the end of injection for the second tracer test with change in hysteresis value and chase water injection: (a) Without injecting, (b) 30 minutes, (c) 3 hours and (d) 12 hours.

mole fraction in the gaseous and aqueous phases as a function of distance, the furthest distance from the injection well that Xenon has travelled at the end of the tracer injection stages for the two tests is about 3 m. At this distance the formation is fully water saturated in the two tracer tests (even after the CO_2 injection in the second test).

Regarding the results illustrated in Figs. 7 and 8, which show the gas saturation versus distance and time, respectively, for a system with critical gas saturation after hysteresis value of 0.2, it can be seen from the figures that the system has reached the highest gas saturation delineated by the drainage curve (0.7) at the end of the injection period.

The plot in Fig. 8, illustrates the gas saturation versus time during production when all the mobile CO_2 was withdrawn, and the residually trapped CO_2 zone was established in the formation. Fig. 8 shows that when water is displaced towards the production well, it is unsaturated at distances of 2.45 m and beyond because CO_2 has not reached that distance. As water is travelling towards the well, when it has reached 2.125 m, it has started dissolving more CO_2, as shown in Fig. 9, which illustrates the CO_2 water mole fraction versus distance at the end of injection. At this distance water has dissolved much of the CO_2, which can be seen from the sharp increase in CO_2 water mole fraction from 0 to 0.0114. This is because it is unsaturated and its capacity to dissolve CO_2 is very strong. Whereas, when the water has reached 2.0 m, its ability to dissolve more CO_2 becomes restricted as it is already nearly saturated. This explains the plateau in CO_2 water mole fraction of 0.0114 from 2 m to the near side of the well. Therefore, as water is moving towards the well from a distance of 2 m and beyond, its capacity to dissolve CO_2 becomes very low. Therefore, in Fig. 7, the CO_2 saturation has decreased fastest on the far side from the well.

The application of Eq. (1) in these calculations yielded a calculated residual gas saturation that is within 10% of the input hysteresis value. This confirms that our test design showed that the single pass of the tracer saturated water over the residual CO_2 zone reduced the amount of CO_2 dissolution into the tracer.

4.2 Sensitivity analysis

4.2.1 Change in critical gas saturation value after hysteresis

Interpreting Fig. 10, the changes in the critical gas saturation due to hysteresis during imbibition have affected the tracer arrival times, where the higher the hysteresis value of the critical gas saturation, the greater the delay in the arrival time. The peak in tracer concentration for the scenario with hysteresis value (S_{gr} = 0.2) arrived at the well faster than the peaks in the cases with hysteresis S_{gr} = 0.3 and 0.4. Where, for the case with hysteresis value of 0.2 the tracer concentration peak arrived at time 6.77 days, for cases with hysteresis values 0.3 and 0.4 the peaks have arrived at time 7.27 days and 7.90 days, respectively. Consequently, this change in the peak arrival times has also affected the calculated residual gas saturation using Eq. (1) as illustrated in Table 5. The bigger the time difference between t_1 and t_2, the higher the calculated residual gas saturation.

According to the results in Table 5, which show the

calculated residual gas saturations using Eq. (1), it can be observed that the calculated residual gas saturation in all these sensitivity calculations is the same as the input critical gas saturation after hysteresis values in the simulations. This demonstrates that it is preferable to use the fluid withdrawal method to establish the residually trapped zone as it produced accurate results for the residual gas saturation calculations, which confirms that the design of this scenario works well.

4.2.2 Change in the amount of chase CO_2 saturated water injected

It can be observed from Figs. 11 and 12 that the amount of chase CO_2 saturated water injected has affected the location of the CO_2 front and the trapped gas saturations.

In all scenarios equal sizes of CO_2 slug were injected, but with varying volumes of chase CO_2 saturated water injected after the CO_2 had been injected; this triggered the CO_2 front to travel to different distances, as can be seen from Figs. 12(c) and 12(d). During production, the Xenon has different sizes of CO_2 (saturated) residually trapped zones to travel through and encounters different residual gas saturations (hysteresis values). The design of this test thus requires calculation of the amount of chase CO_2 saturated water to be injected after the CO_2, to determine how far the CO_2 will travel and ensure it travels to the same distance in all cases regardless of the residual gas saturations. However, the optimal choice of volume of CO_2 saturated water to be injected also requires knowledge of what is the expected possible range of residual gas saturations. In our design method we were able to establish the size of chase CO_2 saturated water volume that would work for residual gas saturation ranges between 0.2 and 0.4. We were also able to force the residual CO_2 zone to travel to the same distance and to be the same size for the four scenarios.

The optimal injection of CO_2-saturated water was challenging to achieve. This is because the amount of chase CO_2 saturated water injected after the CO_2 also affects the amount of CO_2 dissolution in the residually trapped zone, and hence the residual gas saturation calculation. When too much CO_2 saturated water is injected after the CO_2, a wrong calculation of the residual gas saturation will result, since the gas saturation in at least some of the near well formation will be below the actual residual gas saturation. Therefore, the "correct" volume of chase CO_2 saturated water must be injected to make sure that the calculated residual gas saturation obtained from the tracer test calculations is accurate.

Also, it is concluded from the four scenarios that it is preferable to either not injecting CO_2-saturated water after injecting the CO_2 and create the residual CO_2 zone through the fluid withdrawal method as in the base case model, or inject only some CO_2-saturated water after CO_2 injection, which is just enough to push the mobile CO_2 away from the well vicinity, and then withdraw the mobile CO_2 from the formation and leave behind the residual CO_2. This is required to ensure that the CO_2 front will always be at the same distance from the well, regardless of the residual gas saturation. However, if too much chase CO_2 saturated water is injected, such that none of the CO_2 is mobile any longer, then the distance to the CO_2 front will be uncertain. Therefore, in our calculations the design of the case where chase CO_2 saturated water was not injected after the CO_2 is optimal and the case when chase CO_2 saturated water was injected for 30 minutes also worked as it produces a calculated residual gas saturation that is close to the input critical gas saturation after hysteresis.

It is concluded that injecting CO_2-saturated chase water after the CO_2 to prevent dissolution of the residually trapped CO_2 and establish the residually trapped zone, as in the scenario when CO_2-saturated water was injected for 12 hours, turned out to be challenging to achieve. Since, the solubility of CO_2 in water decreases with a decrease in pressure, and as there is a reducing pressure profile moving out from the well into the formation, this caused difficulty in ensuring the water was saturated with CO_2 to a given distance from the well without CO_2 evolving out of solution due to the reduction in pressure. If the water is undersaturated with respect to CO_2, when it is displaced out into the formation it will still dissolve CO_2. Thus, it was not actually possible to displace CO_2-saturated water injected to the desired distance from the well. For this reason, it would be better to inject and produce at lower rather than higher rates to minimise pressure changes.

The residual gas saturation is not in fact constant but changes with distance. Since it is a radial system, the rock volume at 0.1 m is smaller than at 5 m. Therefore, at distances closer to the wellbore there will be multiple volume throughput during both gas and chase CO_2 saturated water injection stages, so the rock will be driven first to residual water saturation and then to residual gas saturation. Thus, in the model, closer to the well the system will be driven to the residual gas saturation determined by the input critical gas saturation after hysteresis. However, further from the well the volume throughput of injected fluids will be lower because the rock volume will be greater, and so the residual water and then gas saturations may not be reached.

It also should be mentioned that in all the numerical experiments more than 99% of the injected tracer is recovered. This is because even though some of the tracer partitions into the gas phase as it contacts it, the gas phase is immobile, and thus multiple pore volumes of water with no tracer flows past it, the tracer partitions back into the mobile aqueous phase. Furthermore, this partitioning back into the aqueous phase is accelerated by the fact that the CO_2 itself is also dissolving into the aqueous phase, and so the volume of gas itself is shrinking-further forcing the tracer back into the aqueous phase. Over the time of the test the system pressure did not change much so the CO_2 solubility did not change as much, but as a function of distance from the well the pressure might change a little and so the solubility of CO_2 may vary.

There are many field and numerical parameters that contribute to uncertainty in the estimation of residual gas saturation using the single well tracer test. Some of the potential uncertainties include porosity, permeability heterogeneity, and subsurface conditions such as water salinity, initial pressure, and initial temperature. Large variations in reservoir porosity and permeability, may have an impact on the estimation of the residual gas saturation. This is because fluid distribution within the reservoir is governed by the permeability and porosity, which hence affect dispersion and partitioning of fluids, all

of which may influence the residual gas saturation estimate. In heterogenous reservoirs in higher permeability layers, the tracer will be pushed farther away from the wellbore than in the lower permeability layers, and thus the tracer has farther distance to travel to return to the well. This will have an impact on the breakthrough tracer concentration curve, and hence may affect the accuracy of the single well tracer test results. This can be reduced or removed by repeating the same tracer test with taking into consideration various heterogeneity levels. Future work should consider these factors that increase complexity. The distribution of the tracer between CO_2 and brine is governed by the partition coefficient value. Subsurface conditions will affect the partition coefficient of the tracers and CO_2/water. The partition coefficient increases with increasing salinity and temperature and reduces with increasing pressure and thus affect the residual gas saturation calculations. Therefore, understanding the parameters that are affecting the partitioning coefficients in advance will significantly reduce the uncertainties of single well tracer test in the field. In addition, these types of component transport calculations are always affected by numerical dispersion. To compensate for that a fine grid cell size of 0.005 m was used, but further refinement could be considered in future work to improve accuracy.

The pros the numerical experiments developed in this study include the fact that with the numerical model it is possible to run multiple of sensitivity studies and estimate what range of residual saturations a particular set of observed data in the field might represent. This numerical experiment will help in evaluating the error in the interpretation of the field data. It will also help in identifying what is the optimal design of tracer test that will give the most successful results.

Other pros include the fact that the impact of the reservoir heterogeneity degree on the tracer test results can be tested in the model. Different models can be run ranging from completely homogeneous to greatly heterogenous formations to evaluate its impact on the results.

The cons of the numerical experiments include that in real reservoir formations there will be heterogeneity of permeability and heterogeneity of residual gas saturations, and so the estimated residual CO_2 saturation is just a single average value. In the model the complexity of all these heterogeneities cannot be captured because there are not enough data known to be able to populate the model to represent the heterogeneity of the formation in the model with a high degree of accuracy, and therefore the model is doing some averaging. However, this test method provides a single critical gas saturation value so the level of data resolution in the model is similar to the data resolution that comes from a field test.

5. Conclusions

This study uses simulation modelling to investigate the applicability of using an alternative single well tracer test design, which involved a single pass of the tracer saturated water over the residual CO_2 zone, with the aim of reducing the amount of CO_2 dissolution into the tracer to produce clear results of the residual gas saturation. The below conclusions can be made from the numerical tracer tests.

1) The obtained results from the base case scenario indicated that the application of the single well tracer test technique using our design method has limited the dissolution of the residual CO_2. The second observation is that the application of Eq. (1) in our experiments yielded a calculated residual gas saturation that is within 10% of the input critical gas saturation (after hysteresis) value.
2) It was also observed from the base case that the tracer breakthrough curve is sensitive to residual gas saturation because during production part of the tracer from the second tracer test has partitioned into the CO_2 phase and become immobile, and thus was not produced back as quickly as in the case where there was no injected gas. These results confirm that our design method agree with the results obtained from previous studies (e.g., Zhang et al. (2011)).
3) Sensitivity study results showed that the arrival times of the tracer peaks, and hence the calculated residual gas saturations, are very sensitive to the input hysteresis value of residual gas saturation in the model. The higher the hysteresis value the more the delay in the arrival times of the peaks. Consequently, the higher the residual gas saturation.
4) Changing the volume of chase CO_2 saturated water injected after the CO_2 made the CO_2 front to travel to different distances from the well, and consequently the Xenon had different size of CO_2 residually trapped zones to travel through when it is back produced and encounters different residual gas saturations (hysteresis values). Therefore, it is critical to calculate in advance the correct amount of chase CO_2 saturated water to be injected after the CO_2, to determine how far the CO_2 will travel and ensure it travels to the same distance in all scenarios regardless of the residual gas saturation.
5) Changing the amount of chase CO_2 saturated water injected after the CO_2 has affected the amount of the CO_2 dissolved, and thus the residual gas saturation calculations. Wrong residual gas saturation results were obtained from the case when too much CO_2 saturated water was injected, because the gas saturation in the near wellbore region was below the residual gas saturation. Consequently, the correct amount of CO_2 saturated water must be injected to ensure that the calculated residual gas saturations from the tracer tests are representative of the actual residual gas saturation.
6) The optimal injection of CO_2-saturated water to prevent the dissolution of the residually trapped CO_2 and establish the residually trapped zone was challenging to achieve, and therefore using the fluid withdrawal method was more robust to establish the residually trapped zone. This is because of the dependency of solubility on pressure, and since there is a pressure profile decreasing while moving out into the system, consequently it was not possible to displace CO_2-saturated water injected to the desired distance from the well without CO_2 evolving out of solution because of pressure reduction.

7) The optimal design of the tracer tests, particularly the volumes of the various stages, requires some a priori knowledge of the system to be characterised; and sensitivity calculations to ensure a test design that is robust in the face of the uncertainties is important.
8) The calculated residual gas saturation is representative of only a small volume of the overall reservoir (that volume closest to the well), and it will be an average over the entire completion interval, which may in reality consist of multiple heterogeneous layers.
9) Overall, even though modelling these tracer experiments has produced a good estimation of the residual gas saturation, the uncertainties and challenges in modelling are high and this means that small changes in system parameters, such as in numerical controls (in the model), hysteresis value and chase CO_2 saturated water volume injected (in the model and in reality) may lead to inaccurate results.

Acknowledgements

The Libyan Ministry of Education are thanked for sponsoring Masra Awag. CMG are thanked for use of the GEM software in this study. Energi Simulation are thanked for supporting the Chair in CCUS and Reactive Flow Simulation held by Eric Mackay.

Conflict of interest

The authors declare no competing interest.

References

Assayag, N., Matter, J., Ader, M., et al. Water-rock interactions during a CO_2 injection field-test: Implications on host rock dissolution and alteration effects. Chemical Geology, 2009, 265(1-2): 227-235.

CMG, GEM. Computer Modelling Group Ltd, 2020.

Dance, T., Paterson, L. Observations of carbon dioxide saturation distribution and residual trapping using core analysis and repeat pulsed-neutron logging at the CO_2CRC Otway site. International Journal of Greenhouse Gas Control, 2016, 47: 210-220.

Doughty, C., Freifeld, B., Trautz, R. Site characterization for CO_2 geologic storage and vice versa: The Frio brine pilot, Texas, USA as a case study. Environmental Geology, 2007, 54: 1635-1656.

Heilweil, V., Kip Solomon, D., Perkins, K., et al. Gas-partitioning tracer test to quantify trapped gas during recharge. Ground Water, 2004, 42(4): 589-600.

Istok, J. D., Field, J. A., Schroth, M. H., et al. Single-well "push-pull" partitioning tracer test for NAPL detection in the subsurface. Environmental Science and Technology, 2002, 36(12): 2708-2716.

Joodaki, S., Moghadasi, R., Basirat, F., et al. Model analysis of CO_2 residual trapping from single-well push pull test-Heletz, Residual Trapping Experiment II. International Journal of Greenhouse Gas Control, 2020a, 101: 103134.

Joodaki, S., Yang, Z., Bensabat, J., et al. Model analysis of CO_2 residual trapping from single-well push pull test based on hydraulic withdrawal tests-Heletz, residual trapping experiment I. International Journal of Greenhouse Gas Control, 2020b, 97: 103058.

Kim, Y., Kim, J., Son, B., et al. A single well push-pull test method for in situ determination of denitrification rates in a nitrate-contaminated groundwater aquifer. Water Science and Technology, 2005, 52(8): 77-86.

Krevor, S., Blunt, M., Benson, S., et al. Capillary trapping for geologic carbon dioxide storage-From pore scale physics to field scale implications. International Journal of Greenhouse Gas Control, 2015, 40: 221-237.

LaForce, T., Ennis-King, J., Boreham, C., et al. Residual CO_2 saturation estimate using noble gas tracers in a single-well field test: The CO_2CRC Otway project. International Journal of Greenhouse Gas Control, 2014, 26: 9-21.

Matter, J. M., Takahashi, T., Goldberg, D. Experimental evaluation of in situ CO_2-water-rock reactions during CO_2 injection in basaltic rocks: Implications for geological CO_2 sequestration. Geochemistry, Geophysics, Geosystems, 2007, 8(2): 1-19.

Metz, B., Davidson, O. IPCC Special Report on Carbon Dioxide Capture and Storage. Cambridge and New York, USA, Cambridge University Press, 2005.

Myers, M., Stalker, L., Ross, A., et al. Method for the determination of residual carbon dioxide saturation using reactive ester tracers. Applied Geochemistry, 2012a, 27(10): 2148-2156.

Myers, M., White, C., Stalker, L., et al. Literature review of tracer partition coefficients. EP01061231, 2012b.

Nelson, N., Brusseau, M., Carlson, T., et al. A gas-phase partitioning tracer method for the in situ measurement of soil-water content. Water Resources Research, 1999, 35(12): 3699-3707.

Niemi, A., Bear, J. Geological Storage of CO_2 in Deep Saline Formations. Dordrecht, Netherlands, Springer, 2017.

Niemi, A., Bensabat, J., Shtivelman, V., et al. Heletz experimental site overview, characterization and data analysis for CO_2 injection and geological storage. International Journal of Greenhouse Gas Control, 2016, 48: 3-23.

Niemi, A., Jacob, B., Joodaki, S., et al. Characterizing CO_2 residual trapping in-situ by means of single-well push-pull experiments at Heletz, pilot injection site-experimental procedures and results of the experiments. International Journal of Greenhouse Gas Control, 2020, 101: 103129.

Paterson, L., Boreham, C., Bunch, M., et al. The CO_2CRC Otway stage 2b residual saturation and dissolution test: Test concept, implementation and data collected. Milestone Report to ANLEC, 2011.

Paterson, L., Boreham, C., Bunch, M., et al. Overview of the CO_2CRC Otway residual saturation and dissolution test. Energy Procedia, 2013, 37: 6140-6148.

Rasmusson, K., Rasmusson, M., Fagerlund, F., et al. Analysis of alternative push–pull-test-designs for determining in

situ residual trapping of carbon dioxide. International Journal of Greenhouse Gas Control, 2014, 27: 155-168.

Tomich, J., Dalton, R., Deans, H., et al. Single-well tracer method to measure residual oil saturation. Journal of Petroleum Technology, 1973, 25(2): 211-218.

Xue, Z., Tanase, D., Watanabe, J. Estimation of CO_2 saturation from time-lapse CO_2 well logging in an onshore aquifer, Nagaoka, Japan. Exploration Geophysics, 2006, 37(1): 19-29.

Zhang, Y., Freifeld, B., Finsterle, S., et al. Single-well experimental design for studying residual trapping of supercritical carbon dioxide. International Journal of Greenhouse Gas Control, 2011, 5(1): 88-98.